Therapeutic Protein PEPylation: The Helix of Nonfouling Synthetic Polypeptides Minimizes Antidrug Antibody Generation

Yingqin Hou,[†] Yu Zhou,[†] Hao Wang,[†] Jialing Sun,[†] Ruijue Wang,[†] Kai Sheng,[†] Jingsong Yuan,[†] Yali Hu,[‡] Yu Chao,[§] Zhuang Liu,[§] and Hua Lu*,[†]

[†]Beijing National Laboratory for Molecular Sciences, Center for Soft Matter Science and Engineering, Key Laboratory of Polymer Chemistry and Physics of Ministry of Education, College of Chemistry and Molecular Engineering, Peking University, Beijing 100871, People's Republic of China

[‡]Peking-Tsinghua Center for Life Sciences, Peking University, Beijing 100871, People's Republic of China

[§]Institute of Functional Nano & Soft Materials (FUNSOM), Collaborative Innovation Center of Suzhou Nano Science and Technology, Soochow University, Suzhou, Jiangsu 215123, China

S *Supporting Information*

ABSTRACT: Polymer conjugation is a clinically proven approach to generate long acting protein drugs with decreased immune responses. Although poly(ethylene glycol) (PEG) is one of the most commonly used conjugation partners due to its unstructured conformation, its therapeutic application is limited by its poor biodegradability, propensity to induce an anti-PEG immune response, and the resultant accelerated blood clearance (ABC) effect. Moreover, the prevailing preference of unstructured polymers for protein conjugation still lacks strong animal data support with appropriate control reagents. By using two biodegradable synthetic polypeptides with similar structural compositions (L-P(EG$_3$Glu) and DL-P(EG$_3$Glu)) for site-specific protein modification, in the current study, we systematically investigate the effect of the polymer conformation on the in vivo pharmacological performances of the resulting conjugates. Our results reveal that the conjugate L$_{20K}$-IFN, interferon (IFN) modified with the helical polypeptide L-P(EG$_3$Glu) shows improved binding affinity, in vitro antiproliferative activity, and in vivo efficacy compared to those modified with the unstructured polypeptide analogue DL-P(EG$_3$Glu) or PEG. Moreover, L$_{20K}$-IFN triggered significantly less antidrug and antipolymer antibodies than the other two. Importantly, the unusual findings observed in the IFN series are reproduced in a human growth hormone (GH) conjugate series. Subcutaneously infused L$_{20K}$-GH, GH modified with L-P(EG$_3$Glu), evokes considerably less anti-GH and antipolymer antibodies compared to those modified with DL-P(EG$_3$Glu) or PEG (DL$_{20K}$-GH or PEG$_{20K}$−GH). As a result, repeated injections of DL$_{20K}$-GH or PEG$_{20K}$-GH, but not L$_{20K}$-GH, result in a clear ABC effect and significantly diminished drug availability in the blood. Meanwhile, immature mouse bone marrow cells incubated with the helical L$_{20K}$-GH exhibit decreased drug uptake and secretion of proinflammatory cytokines compared to those treated with one of the other two GH conjugates bearing unstructured polymers. Taken together, the current study highlights an urgent necessity to systematically reassess the pros and cons of choosing unstructured polymers for protein conjugation. Furthermore, our results also lay the foundation for the development of next-generation biohybrid drugs based on helical synthetic polypeptides.
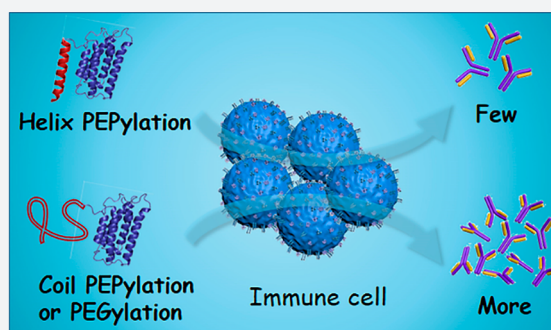
INTRODUCTION

Therapeutic proteins are important biologics that frequently exhibit high potency and selectivity. However, their clinical use has been hampered by their rapid renal clearance, susceptibility to proteolysis, and strong immunogenicity.[1−3] Particularly, the generation of antidrug antibodies (ADAs) has been a serious hurdle for many protein drugs.[4] One proven strategy to overcome these limitations is to covalently conjugate the protein of interest to polymers such as poly(ethylene glycol) (PEG), a process known as PEGylation, which can lead to significantly increased hydrodynamic volume, in vivo stability, and circulation half-life.[5−10] However, there is mounting evidence that PEGylated proteins tend to show poorer binding

affinity and biological activity than their unconjugated equivalents.[11,12] Furthermore, although one of the initial purposes of PEGylation is for reduced ADA generation, PEG is known to elicit anti-PEG antibodies that adversely accelerate the blood clearance of the PEGylated proteins or nanoparticles, known as the ABC effect. As evidence, reduction in the therapeutic efficacy of many PEGylated proteins, such as uricase, asparaginase, and interferon (IFN), has been found to strongly correlate with the occurrence of the anti-PEG immune response that they induce.[13] More worrisome is the fact that

Scheme 1. Site-Specific Conjugation of Synthetic Polypeptides or PEG To Engineer Therapeutic Proteins (IFN and GH) via Native Chemical Ligation
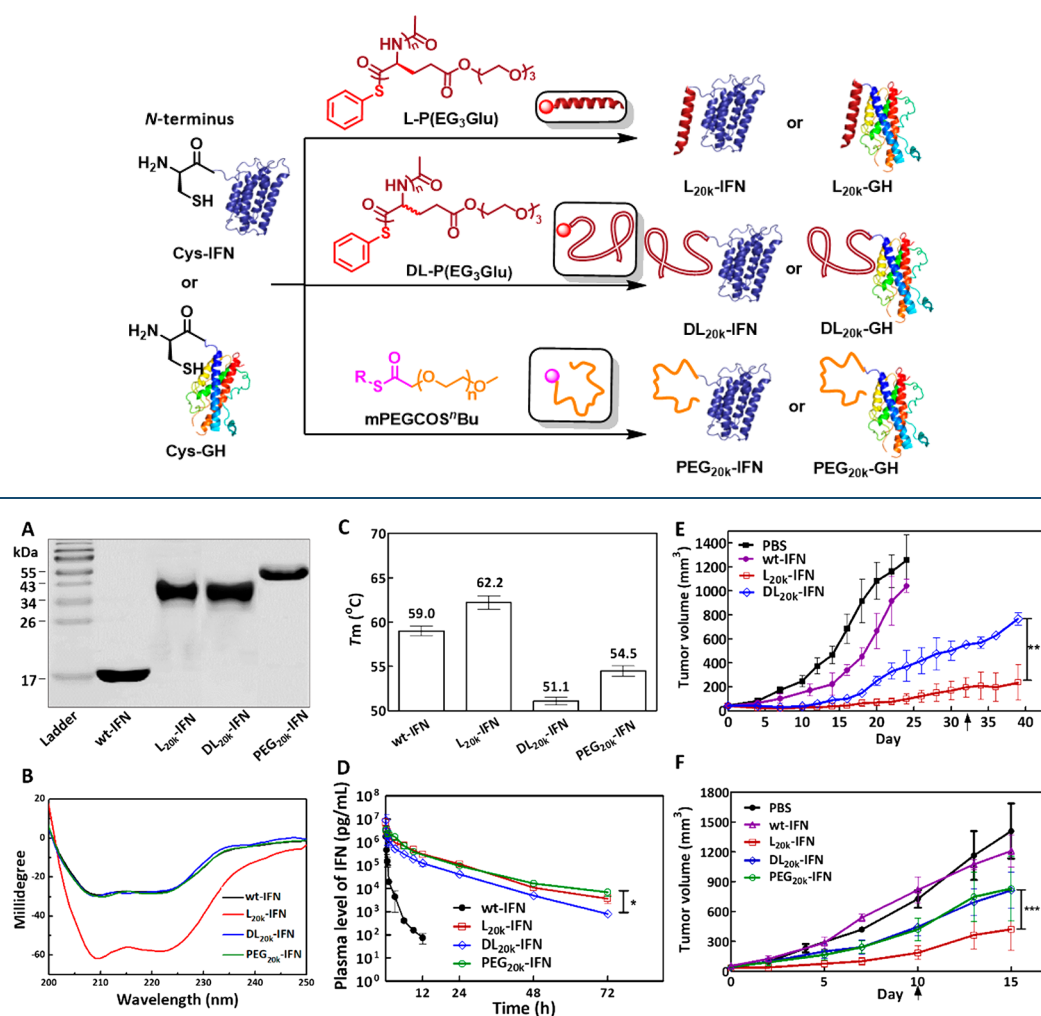

Figure 1. Characterization and in vivo pharmacological performances of various IFN conjugates. (A) SDS-PAGE gel, stained by Coomassie blue. (B) Circular dichroism (CD) spectroscopy. (C) Melting temperature (T_m) measured by thermofluoro assay. (D) In vivo pharmacokinetics (i.v. injection) of wt-IFN ($n = 6$), L_{20K}-IFN ($n = 6$), and DL_{20K}-IFN ($n = 6$), and PEG_{20K}−IFN ($n = 3$). (E−F) Tumor growth inhibition curves. BALB/C-nu mice bearing s.c. OVCAR-3 xenograft (E) or patient-derived xenograft (PDX) tumors (F) were i.v. injected with PBS saline or one of the IFN-based drugs ($n = 7$ each); treatments began on day 0, and the black arrows indicate ending of the treatments. The total injection numbers are six in E and three in F. Data are expressed as mean ± SD. P value is determined by two-way ANOVA (Bonferroni post-test) analysis: $*p < 0.05$, $**p < 0.01$, $***p < 0.001$.

the percentage of healthy adults carrying pre-existing anti-PEG antibodies has increased sharply from 0.2% to 42% during the past three decades, likely because of their daily exposure to PEG-containing commodities.[13] Thus, a pressing need in this field is seeking new polymers beyond PEGylation.

In recent years, researchers have investigated a wide range of alternative conjugation partners,[14] including zwitterionic polymers,[15,16] polyglycerol,[17] glycopolymers,[18] and oligo-EGylated poly(meth)acrylates,[19,20] with varying degrees of success. Despite the potential of these methods, the lack of biodegradability has remained a central problem.[5] Synthetic polypeptides have been increasingly considered as a biodegradable and biocompatible alternative to PEG with great clinical promise.[21−25] There has been evidence that the genetic fusion of therapeutic proteins/peptides to intrinsically disordered polypeptides, such as XTEN, PAS, and elastin-like polypeptides (ELP), can lead to improved pharmacological performance in vivo.[26−32] We envisage that the chemical

modification of proteins by synthetic polypeptides, which we call PEPylation, could open up enormous possibilities.[33−35] Particularly, the chemical diversity of synthetic polypeptides has been greatly expanded by incorporating noncanonical amino acids via ring-opening polymerization (ROP) of α-amino acid N-carboxyanhydrides (NCA) and utilizing D-amino acids.[20] Notably, during the preparation of this manuscript, Jiang et al. reported the nonspecific grafting of zwitterionic polypeptides to uricase,[36] which showed extraordinarily low immunogenicity and outstanding safety profile in vivo. Their work underscored the exceptional clinical potential of PEPylation.

When surveying the aforementioned polymers for protein modification, one can easily draw the conclusion that unstructured and flexible polymers (e.g., PEG) have long been the preferred conjugation partners due to their ability to augment the hydrodynamic volume of the modified protein and provide an excellent stealth effect that minimizes renal

Table 1. In Vitro Binding, Anti-Proliferative Activity, and in Vivo Pharmacokinetics[a] of wt-IFN and Various IFN Conjugates

sample	IC50 (pg/mL)	K_D (nM)	elimination half-life (h)[b]	AUC$_{0-t}$ ((μg/mL)*h)[c]	V_d (mL)[d]	CI (mL/h)
wt-IFN	8.5 ± 1.4	1.0	0.5 ± 0.1	0.4 ± 0.1		125 ± 21.8
L$_{20k}$-IFN	36.0 ± 1.3	5.8	9.6 ± 0.6	15.5 ± 2.2	167 ± 49	3.2 ± 0.6
DL$_{20k}$-IFN	160 ± 4	19.6	7.8 ± 0.3	8.6 ± 0.7	239 ± 49	5.8 ± 0.7
PEG$_{20k}$-IFN	190 ± 10	15.9	9.8 ± 1.9	17.0 ± 3.0	161 ± 25	2.9 ± 0.4

[a]Dose: 50 μg/rat on IFN base. [b]Elimination half-life: Time points used to calculate $t_{1/2}\beta$ are 3−12 h (wt IFN), 12−72 h (all conjugates). [c]AUC calculated by logarithmic trapezoidal rule up to 12 h (wt-IFN),72 h (L$_{20K}$-IFN, DL$_{20K}$-IFN, and PEG$_{20K}$−IFN). [d]V_d calculated at 12 h after intravenous injection. [e]Data are expressed as mean ± SD.
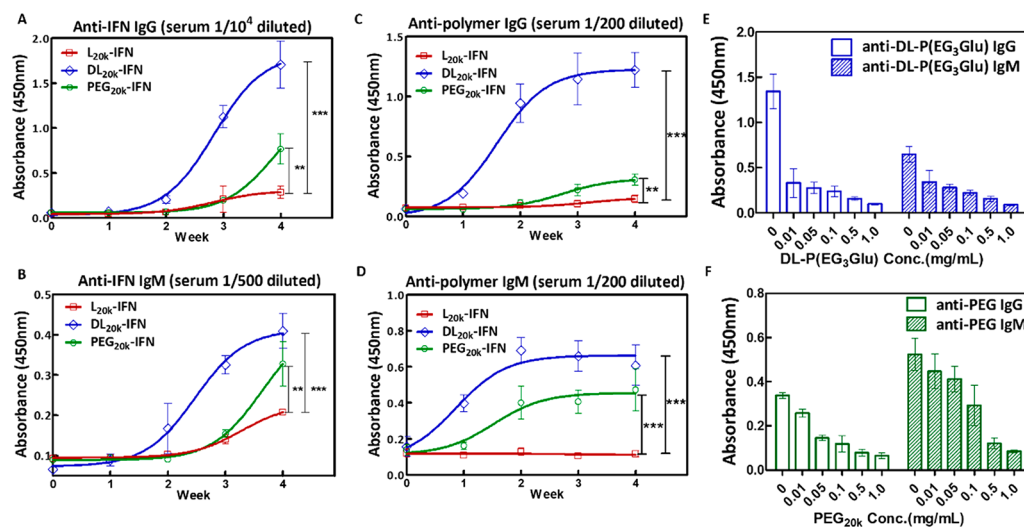

Figure 2. In vivo immune responses triggered by IFN conjugates. (A−B) Anti-IFN IgG (A) and IgM (B) contents in the sera measured by ELISA; the plates were coated with wt-IFN and then incubated with 10^4-fold (for IgG) or 500-fold (for IgM) prediluted sera in PBS. (C−D) Antipolymer IgG (C) and IgM (D) contents in the sera immunized with various polymer-IFN conjugates; for each polymer-of-interest, the ELISA plates were coated with the corresponding polymer-GH conjugate. (E−F) Antipolymer ELISA assays using free DL-P(EG3Glu) (E) or PEG (F) as the competition agent; sera immunized with DL$_{20K}$-IFN or PEG$_{20K}$−IFN (week 4) were prediluted 200-fold and incubated with the corresponding free polymer at gradient concentrations. Immunization protocol: rats were s.c. infused with L$_{20K}$-IFN, DL$_{20K}$-IFN, or PEG$_{20K}$−IFN at a weekly dose 0.2 mg/kg for 4 weeks; sera were drawn from the rats ($n = 3$) every week starting from week 0. For ELISA analysis, after sera incubation and washing, all plates were incubated with antimouse IgG-HRP or IgM-HRP, and analyzed by TMB solution (CWBIO). TWEEN was excluded from the buffers in all antipolymer ELISA studies. Data are expressed as mean ± SD P value is determined by two-way ANOVA (Bonferroni post-test) analysis: *$p < 0.05$, **$p < 0.01$, ***$p < 0.001$.

filtration and immune attack. Following the same principle, elementary amino acids are carefully selected in the design of XTEN to ensure an unstructured conformation and absence of helical structures.[26] However, it is surprising that there have been very few studies that attempt to investigate whether the conformation, particularly the helix, of the polymer has any effect on the in vivo performance of the protein that it modifies. One practical challenge resides in the difficulty of generating protein conjugates that only differ in the conformation of the attached polymers to ensure a fair comparison. We reason that synthetic polypeptides offer an ideal solution to this problem as their secondary conformations (e.g., helix and coil) can be easily manipulated by switching the chirality of the monomers without altering the overall chemical composition.[37,38]

RESULTS

Synthesis and Characterization of Different IFN−Polymer Conjugates. Recombinant IFN, an antiviral and antitumor cytokine, was selected as our first model drug. For a fair comparison, we synthesized two chemically similar but conformationally varied polypeptides (Scheme 1).[34,35] Specifically, monomer γ-(2-(2-(2-methoxyethoxy)ethoxy)ethyl L-

glutamate NCA[39] (L-EG$_3$GluNCA) was polymerized by trimethylsilyl phenylsulfide (PhS-TMS) to yield phenyl thioester-functionalized L-P(EG$_3$Glu) (Scheme 1). Similarly, DL-P(EG$_3$Glu) was produced from a racemic mixture of DL-EG$_3$GluNCA. The molecular weights (MW) of both polymers were carefully controlled to be ∼20 kDa, in line with many clinically approved PEG conjugates. Gel permeation chromatography (GPC) indicated that the two polymers had a similar MW ≈ 22−23 kDa and narrow dispersity ($Đ$) below 1.05 (Figure S1). ^{1}H NMR spectroscopy showed that the two polymers differed in the chemical shift of the α-H due to the different α-C chirality (Figure S2). As expected, circular dichroism (CD) spectroscopy revealed that α-helices constituted more than 90% of L-P(EG$_3$Glu), whereas DL-P(EG$_3$Glu) was unstructured as design (Figure S3). Subsequently, we conjugated each synthetic polypeptide to an IFN mutant bearing a N-terminal cysteine (Cys-IFN) via native chemical ligation, thereby forming two PEPylated IFNs denoted as L$_{20K}$-IFN and DL$_{20K}$-IFN (Scheme 1). We also generated PEG$_{20K}$-IFN as a positive control by attaching a thioester-functionalized PEG (MW ≈ 20 kDa) to IFN via the same method (Scheme 1 and Figure S4).

All purified IFN conjugates exhibited a narrow size distribution based on SDS-PAGE analysis (Figure 1A). L$_{20K}$-
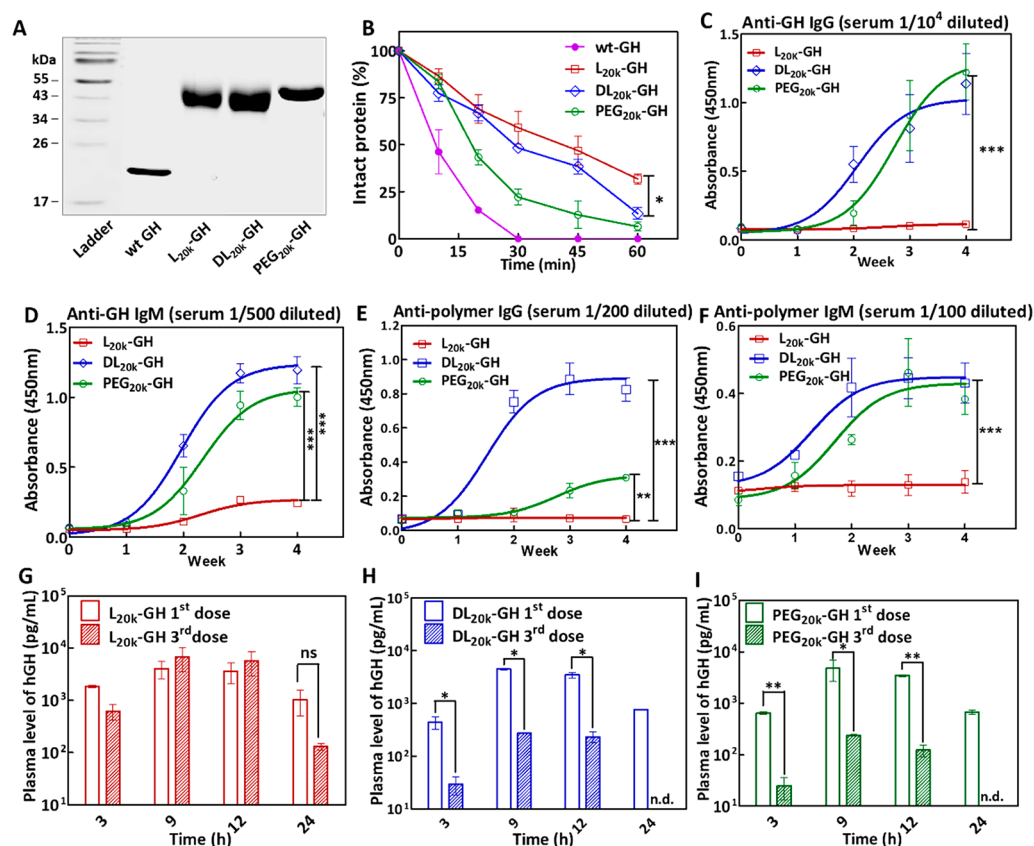
Figure 3. In vivo immune responses triggered by GH conjugates. (A) SDS-PAGE gel analysis. (B) Trypsin degradation curves. (C−D) Anti-GH IgG (C) and IgM (D) contents in the sera measured by ELISA; the plates were coated with wt-GH and then incubated with 10^4-fold (for IgG) or 500-fold (for IgM) prediluted sera in PBS. (E−F) Antipolymer IgG (E) and IgM (F) contents in the sera immunized with polymer-GH conjugates; for each polymer of interest, the ELISA plates were coated with the corresponding polymer−IFN conjugate and then incubated with the 200-fold prediluted sera. Immunization protocol: rats were s.c. infused with L_{20K}-GH, DL_{20K}-GH, or PEG_{20K}-GH at a weekly dose 0.2 mg/kg for 4 weeks; sera were drawn from the rats ($n = 3$) every week starting from week 0. For ELISA analysis, after sera incubation and washing, all plates were incubated with antimouse IgG-HRP or IgM-HRP, and analyzed by TMB solution (CWBIO). TWEEN was excluded from the buffers in all antipolymer ELISA studies. (G−I) Blood GH contents at selected time points, measured by ELISA, after the first and third s.c. injections of L_{20K}-GH (G), DL_{20K}-GH (H), or PEG_{20K}−GH (I). Data are expressed as mean ± SD. P value is determined by two-way ANOVA (Bonferroni post-test) analysis: $*p < 0.05$, $**p < 0.01$, $***p < 0.001$.

IFN and DL_{20K}-IFN shared an almost identical apparent MW, whereas PEG_{20K}-IFN appeared to electrophoresize slightly slower than its PEPylated counterparts but was still comparable (Figure 1A). CD spectroscopy suggested that PEG_{20K}-IFN and DL_{20K}-IFN were similar in helicity as wt-IFN, whereas L_{20K}-IFN produced a stronger helical signal intensity (Figure 1B). A thermofluoro assay[39] indicated that L_{20K}-IFN possessed a higher T_m, and therefore greater thermostability, than both DL_{20K}-IFN and PEG_{20K}−IFN (Figure 1C). All conjugates were shown to be significantly more resistant to proteolysis than wt-IFN in trypsin digestion assays (Figure S5). Surface plasmon resonance (SPR) found the K_D values for the binding of L_{20K}-IFN, DL_{20K}-IFN, and PEG_{20K}−IFN to human IFNAR2 were 5.8, 19.6, and 15.9 nM, respectively (Table 1 and Figure S6). Thus, L_{20K}-IFN appeared to be ∼3−4 fold more efficient in its receptor interaction than DL_{20K}-IFN or PEG_{20K}−IFN. Consistently, an in vitro viability assay demonstrated that the IC_{50} values of L_{20K}-IFN, DL_{20K}-IFN, and PEG_{20K}−IFN against Daudi cells, an IFN-sensitive human cancer cell line, were 36, 160, and 190 pg/mL, respectively (Table 1). This implied that L_{20K}-IFN could induce a significantly more potent antitumor effect than DL_{20K}-IFN or PEG_{20K}−IFN does.

In Vivo Pharmacological Performances of IFN Conjugates. We next measured the pharmacokinetic parameters of the IFN variants in female Sprague−Dawley rats. As shown in Figure 1D and Table 1, the elimination half-lives ($t_{1/2}\beta$) of L_{20K}-IFN, DL_{20K}-IFN, and PEG_{20K}−IFN were 9.6, 7.8, and 9.8 h, respectively, all significantly longer than the 0.5 h $t_{1/2}\beta$ of wt-IFN. Interestingly, L_{20K}-IFN was slightly but consistently longer-lived than DL_{20K}-IFN (P value < 0.05; reproducible in at least two independent experiments with different batches of materials). This was further evidenced by the greater AUC of L_{20K}-IFN than that of DL_{20K}-IFN (Table 1). The in vivo efficacy of the conjugates was further evaluated in two murine models, one bearing OVCAR-3 tumor xenografts and the other xenografts derived from a prostate cancer patient (PDX) (see Materials and Methods). In both cases, administration of L_{20K}-IFN, which carried the helical L-P(EG₃Glu), led to significantly slower tumor growth (Figure 1A). The superior antitumor efficacy was further confirmed by the reduced tumor cell proliferation activity according to K_i-67 staining (Figure S7). No body weight loss was observed in either model during the treatment with L_{20K}-IFN, suggesting that the drug was well tolerated under the regimen that we employed (Figure S8).
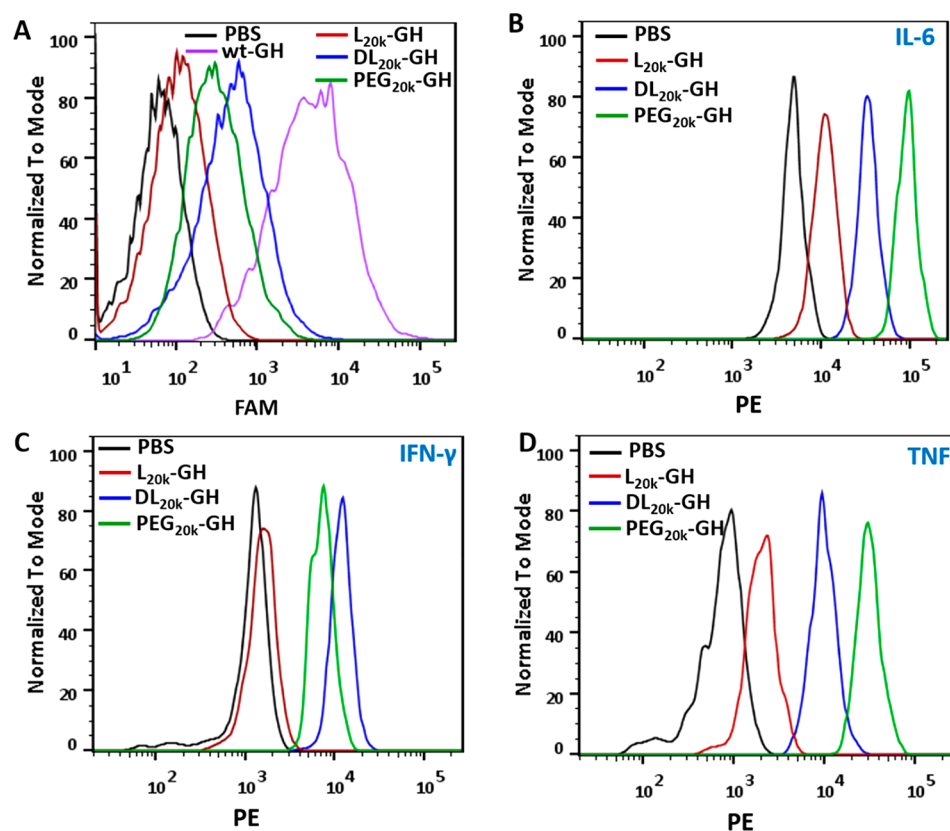
Figure 4. BMDC internalization and activation. (A) Flow cytometry analysis of BMDC internalization of various FAM-labeled GH conjugates. (B−D) Flow cytometry analysis of proinflammatory cytokines secretion: IL-6 (B), IFN-γ (C), and TNF (D). Freshly separated naïve BMDCs were ex vivo incubated in 24-well plate (5×10^5 cells/well) for 6 days and treated with conjugates for 12 h (A) or 24 h (B−D) at 37 °C. The cytokines in the medium were measured with CBA Mouse Inflammation kit following manufacturer's protocol. The PBS-treated BMDCs were served as controls.

Antibody Generation Triggered by IFN Conjugates. To investigate the immune response of the conjugates, Sprague−Dawley rats were randomly grouped and subcutaneously administrated with L_{20K}-IFN, DL_{20K}-IFN, or PEG_{20K}−IFN at a weekly dose of 0.2 mg/kg. Interestingly, sera from the mice immunized with L_{20K}-IFN showed significantly lower levels of anti-IFN IgG and IgM than those receiving DL_{20K}-IFN or PEG_{20K}−IFN (Figure 2A−B). Serial dilution of sera from week 4 revealed that L_{20K}-IFN produced ∼50−100 fold lower anti-IFN IgG and ∼5−10 fold lower IgM titers than those immunized with DL_{20K}-IFN or PEG_{20K}−IFN (Figure S9). In addition, injection with DL_{20K}-IFN or PEG_{20K}−IFN appeared to also induce a detectable amount of antipolymer antibodies, particularly IgM (Figure 2C−D). The specificity of the antipolymer antibodies in DL_{20K}-IFN and PEG_{20K}−IFN sera was further validated by the corresponding polymer competition (Figure 2E−F). Strikingly, we discovered that L_{20K}-IFN exhibited almost no detectable effect on the serum level of antipolymer IgG or IgM in the immunized rats.

Synthesis of and Immune Responses Triggered by Different GH−Polymer Conjugates. To test whether our findings observed in the IFN conjugates were also applicable to other therapeutic proteins, we selected human growth hormone (GH)[41,42] as our second example and engineered the protein with a N-terminal cysteine (Cys-GH), similar to that in Cys-IFN. We next covalently tethered L-P(EG₃Glu), DL-P(EG₃Glu), and PEG separately to Cys-GH to generate three conjugates denoted as L_{20K}-GH, DL_{20K}-GH, and PEG_{20K}−GH,

respectively (Scheme 1 and Figure 3A). Trypsin digestion revealed that L_{20K}-GH was significantly more resistant to proteolysis than DL_{20K}-GH and PEG_{20K}-GH (Figure 3B). Furthermore, injection with L_{20K}-GH provoked substantially less production of anti-GH IgG and IgM antibodies in rats from week 2, compared to treatment with DL_{20K}-GH or PEG_{20K}-GH (Figure 3C−D). Serial dilution of sera from week 4 revealed that L_{20K}-GH produced ∼100 fold lower anti-GH IgG and ∼20-fold lower IgM titers than those immunized with DL_{20K}-GH or PEG_{20K}−GH (Figure S10). The same trend was observed when we measured the levels of antipolymer IgG and IgM following the immunization (Figure 3E−F and Figure S11). To examine the ABC effect, we measured the blood concentration of GH at selected time points after the first and third injection of each conjugate. The results demonstrated that infusions of L_{20K}-GH led to very similar blood levels of GH during the first 12 h and generated almost no ABC effect in 24 h (Figure 3G, statistically insignificant). In sharp contrast, both DL_{20K}-GH and PEG_{20K}−GH caused a characteristic ABC effect after the third injection (Figure 3H−I). In fact, our ELISA kit failed to detect blood GH at 24 h following the administration of DL_{20K}-GH or PEG_{20K}-GH (Figure 3H−I). As a result, the $AUC_{0−24h}$ of L_{20K}-GH were comparable after the first and third injection (100% vs 112%), whereas the $AUC_{0−24h}$ of both DL_{20K}-GH and PEG_{20K}−GH after the third infusion were only ∼6% of those after the first drug infusion (Table S1).

BMDC Uptake and Activation. During antibody production, the antigens are usually internalized, fragmented

in lysosome, and displayed on the cell surface by dendritic cells (DCs) to trigger downstream T cell and B cell response. To understand the different antibody responses triggered by the conjugates, we sought to examine the very first DC internalization step. For this, we incubated the GH conjugates with freshly induced immature mouse bone marrow-derived dendritic cells (BMDCs), which are widely used for the assessment of antigen presenting.[43] Flow cytometric analysis found clear evidence for the internalization of DL_{20K}-GH and PEG_{20K}−GH into BMDCs after 12 h of incubation, whereas the uptake level of L_{20K}-GH was considerably lower (Figure 4A). Consistently, treatment of BMDCs with L_{20K}-GH resulted in appreciably less secretion of proinflammatory cytokines, including interleukine-6 (IL-6, Figure 4B), interferon-γ (IFN-γ, Figure 4C), and tumor necrosis factor (TNF, Figure 4D), compared to the other two GH conjugates carrying unstructured polymers.

DISCUSSION

The conjugation of polymers to a protein has been demonstrated to extend its half-time by increasing its hydrodynamic volume and mitigating the ADA generation.[1] However, the role that the secondary conformation of a polymer plays in the resultant protein conjugate has been very rarely investigated, as unstructured polymers have been the heavily favored choice in past studies. Notably, the polypeptide−uricase conjugate reported by Jiang focused on the zwitterionic side chain without studying the secondary conformation effect.[36] We speculated that peptide-based drugs and biomaterials covalently modified with α-helical polypeptides could exhibit improved proteolytic and thermal stability, binding, as well as other biological functions over those conjugated with disordered polymers.[37,44−47] To ascertain whether this is the case, however, one needs to employ polymers that only differ in conformation. Gratifyingly, controlled NCA ROP and chemoselective labeling collaboratively enabled us to generate protein conjugates that shared almost identical modification sites and MWs, and were attached to nearly the same number of polypeptides with highly similar chemical compositions.[34] As a result, the secondary conformation of the tethered polypeptides became the only major variable. This was corroborated by the GPC curves of the polymers and the narrow size distributions of the resultant conjugates on the SDS-PAGE gel (Figure S1, Figures 1A and 3A). Of note, due to the distinct chemical structures of PEG and our P(EG₃-Glu), the migration of those conjugates in SDS-PAGE gel might not completely correlate their MWs, which is often observed for other polymer modified proteins.

Our results found the helical polypeptide-bearing L_{20K}-IFN to have higher binding affinity and antiproliferative activity in vitro than DL_{20K}-IFN and PEG_{20K}−IFN, both of which were attached to unstructured polymers (Table 1). This could be partially attributed to the less steric hindrance imparted by the rigid helical polypeptides. Moreover, L_{20K}-IFN exhibited significant improvement in circulation half-life and in vivo efficacy compared to DL_{20K}-IFN (Figure 1D). Taken together, these data suggested that the conjugation of a rigid helical polypeptide could improve the blood retention of the modified protein drug without significantly affecting its binding affinity or potency, thereby offering a viable solution to the well-known "PEG dilemma".[11]

Some of the greatest controversies of PEGylation include the insufficient protection of the conjugated proteins from immune recognition and the generation of anti-PEG antibodies.[13,48] In the clinic, the anti-IFN neutralizing antibodies has previously been observed in nonresponding patients and believed to be the major reason for their development of resistance.[49] In this regard, it was remarkable that the administration of L_{20K}-IFN provoked substantially lower production of anti-IFN, as well as antipolymer IgG and IgM, than DL_{20K}-IFN or PEG_{20K}−IFN (Figure 2). Importantly, similar results were also obtained from the GH conjugates, indicating that the benefits we observed were independent of the modified protein (Figure 3). We also synthesized a left-handed helical polypeptide D-P(EG₃Glu) (~23 kDa) and produced two conjugates, D_{20K}-IFN and D_{20K}-GH (data not shown). We discovered that both D_{20K}-IFN and D_{20K}-GH, similar to L_{20K}-IFN or L_{20K}-GH, showed almost no antibody response after repeated administration (data not shown). The results lent further evidence to the generality of the helix effect. Moreover, the above study help ruling out the possibility of D-amino acid-induced antibody production in the cases of DL_{20K}-IFN and DL_{20K}-GH. Although the exact mechanistic role of helicity remains insufficiently explored, a number of reasons may count for the unexpected findings. First of all, the helical L-P(EG₃Glu) seems to provide better antifouling property than DL-P(EG₃Glu) and PEG, and thus minimizing nonspecific internalization with cells and proteins. Our initial investigation provided preliminary evidence of conformation-dependent internalization and activation of immature BMDCs for those examined protein−polymer conjugates. In fact, this helical conformation enhanced antifouling and anticell adhesion was also observed when the polypeptides were anchored on gold surfaces.[50] Second, helical polypeptides are well-known more proteolytic stable (Figure 3B) than those unstructured peptidyl analogues, which may lead to inefficient fragmentation and MHC presentation after BMDC internalization. More rigorous experimental and modeling studies are currently ongoing to fully uncover the molecular mechanism of the unusual helical conformation effect.

CONCLUSIONS

In conclusion, we generated synthetic polypeptides that only differed in conformation and compared their effects on the in vivo therapeutic and immunological properties of the protein drugs to which they were conjugated. Compared with the unstructured DL-P(EG₃Glu) or PEG, the covalent attachment of the helical L-P(EG₃Glu) to therapeutic proteins (namely, IFN and GH) led to substantial improvement in a variety of pharmacological properties, such as binding affinity, stability, and in vivo efficacy. Most interestingly, the helical L-P(EG₃Glu)-conjugated IFN and GH elicited a significantly milder immune response and exhibited a much weaker ABC effect than those modified with unstructured polymers. Thus, the helical nonfouling polypeptides that we employed could be excellent alternatives to PEG for mitigating the antibody response to repeatedly administered therapeutic proteins, though whether similar benefits apply to more immunogenic foreign proteins requires further validation. Moreover, our results suggested that the helical conformation of the synthetic nonfouling polypeptides played an important role in minimizing/delaying this antibody response. Taken together, the current study highlighted an urgent necessity to systematically reassess the pros and cons of choosing unstructured polymers for protein conjugation. Furthermore, our results also

lay the foundation for the development of next-generation biohybrid drugs based on helical synthetic polypeptides.

■ ASSOCIATED CONTENT

ⓢ Supporting Information

The Supporting Information is available free of charge on the ACS Publications website at DOI: 10.1021/acscentsci.8b00548.

GPC curves, ^{1}H NMR, CD spectra, trypsin degradation curves, SPR binding curves, K_i-67 stained images of tumor, relative body weight of mice, antibody titer curves, AUC_{0-24h} of GH-polymer conjugates at first and third dose (PDF)

■ AUTHOR INFORMATION

Corresponding Author
*E-mail: chemhualu@pku.edu.cn.

ORCID ⓞ
Zhuang Liu: 0000-0002-1629-1039
Hua Lu: 0000-0003-2180-3091

Notes
The authors declare no competing financial interest.

■ ACKNOWLEDGMENTS

We thank Prof. Demin Zhou for sharing the plasmid encoding the wt-GH, Prof. Wei Wei for the help of BMDC culturing, and Prof. Richard Lerner, Prof. Xing Chen, Prof. Feng Wang for helpful discussion.

■ REFERENCES

(1) Kontos, S.; Hubbell, J. A. Drug development: longer-lived proteins. *Chem. Soc. Rev.* **2012**, *41* (7), 2686−2695.
(2) Zelikin, A. N.; Ehrhardt, C.; Healy, A. M. Materials and methods for delivery of biological drugs. *Nat. Chem.* **2016**, *8* (11), 997−1007.
(3) Liu, T.; Du, J. J.; Luo, X. Z.; Schultz, P. G.; Wang, F. Homogeneously modified immunoglobulin domains for therapeutic application. *Curr. Opin. Chem. Biol.* **2015**, *28*, 66−74.
(4) Krishna, M.; Nadler, S. G. Immunogenicity to biotherapeutics − the role of anti-drug immune Complexes. *Front. Immunol.* **2016**, *7*, 21.
(5) Pelegri-O'Day, E. M.; Lin, E. W.; Maynard, H. D. Therapeutic protein-polymer conjugates: advancing beyond PEGylation. *J. Am. Chem. Soc.* **2014**, *136* (41), 14323−14332.
(6) Cobo, I.; Li, M.; Sumerlin, B. S.; Perrier, S. Smart hybrid materials by conjugation of responsive polymers to biomacromolecules. *Nat. Mater.* **2015**, *14* (2), 143−159.
(7) White, C. J.; Bode, J. W. PEGylation and dimerization of expressed proteins under near equimolar conditions with potassium 2-pyridyl acyltrifluoroborates. *ACS Cent. Sci.* **2018**, *4* (2), 197−206.
(8) Wilson, P.; Nicolas, J.; Haddleton, D. M. Polymer−protein/peptide bioconjugates. In *Chemistry of Organo-Hybrids*; John Wiley & Sons, Inc.: Hoboken, NJ, 2014; p 466.
(9) Dumas, A.; Spicer, C. D.; Gao, Z.; Takehana, T.; Lin, Y. A.; Yasukohchi, T.; Davis, B. G. Self-liganded Suzuki-Miyaura coupling for site-selective protein PEGylation. *Angew. Chem., Int. Ed.* **2013**, *52* (14), 3916−3921.

(10) Pasut, G.; Veronese, F. M. State of the art in PEGylation: the great versatility achieved after forty years of research. *J. Controlled Release* **2012**, *161* (2), 461−472.
(11) Fishburn, C. S. The pharmacology of PEGylation: Balancing PD with PK to generate novel therapeutics. *J. Pharm. Sci.* **2008**, *97* (10), 4167−4183.
(12) Gauthier, M. A.; Klok, H. A. Polymer-protein conjugates: an enzymatic activity perspective. *Polym. Chem.* **2010**, *1* (9), 1352−1373.
(13) Zhang, P.; Sun, F.; Liu, S. J.; Jiang, S. Y. Anti-PEG antibodies in the clinic: Current issues and beyond PEGylation. *J. Controlled Release* **2016**, *244*, 184−193.
(14) Knop, K.; Hoogenboom, R.; Fischer, D.; Schubert, U. S. Poly(ethylene glycol) in drug delivery: pros and cons as well as potential alternatives. *Angew. Chem., Int. Ed.* **2010**, *49* (36), 6288−6308.
(15) Liu, S. J.; Jiang, S. Y. Chemical conjugation of zwitterionic polymers protects immunogenic enzyme and preserves bioactivity without polymer-specific antibody response. *Nano Today* **2016**, *11* (3), 285−291.
(16) Keefe, A. J.; Jiang, S. Poly(zwitterionic)protein conjugates offer increased stability without sacrificing binding affinity or bioactivity. *Nat. Chem.* **2012**, *4* (1), 59−63.
(17) Frey, H.; Haag, R. Dendritic polyglycerol: a new versatile biocompatible-material. *Rev. Mol. Biotechnol.* **2002**, *90* (3−4), 257−267.
(18) Mancini, R. J.; Lee, J.; Maynard, H. D. Trehalose glycopolymers for stabilization of protein conjugates to environmental stressors. *J. Am. Chem. Soc.* **2012**, *134* (20), 8474−8479.
(19) Liu, M.; Johansen, P.; Zabel, F.; Leroux, J. C.; Gauthier, M. A. Semi-permeable coatings fabricated from comb-polymers efficiently protect proteins in vivo. *Nat. Commun.* **2014**, *5*, 5526.
(20) Gao, W. P.; Liu, W. G.; Mackay, J. A.; Zalutsky, M. R.; Toone, E. J.; Chilkoti, A. In situ growth of a stoichiometric PEG-like conjugate at a protein's N-terminus with significantly improved pharmacokinetics. *Proc. Natl. Acad. Sci. U. S. A.* **2009**, *106* (36), 15231−15236.
(21) Deming, T. J. Synthesis of side-chain modified polypeptides. *Chem. Rev.* **2016**, *116* (3), 786−808.
(22) Talelli, M.; Vicent, M. J. Reduction sensitive poly(l-glutamic acid) (PGA)-protein conjugates designed for polymer masked-unmasked protein therapy. *Biomacromolecules* **2014**, *15* (11), 4168−4177.
(23) Lu, Y. J.; Mbong, G. N. N.; Liu, P.; Chan, C.; Cai, Z. L.; Weinrich, D.; Boyle, A. J.; Reilly, R. M.; Winnik, M. A. Synthesis of polyglutamide-based metal-chelating polymers and their site-specific conjugation to trastuzumab for auger electron radioimmunotherapy. *Biomacromolecules* **2014**, *15* (6), 2027−2037.
(24) Song, Z.; Han, Z.; Lv, S.; Chen, C.; Chen, L.; Yin, L.; Cheng, J. Synthetic polypeptides: from polymer design to supramolecular assembly and biomedical application. *Chem. Soc. Rev.* **2017**, *46* (21), 6570−6599.
(25) Kramer, J. R.; Onoa, B.; Bustamante, C.; Bertozzi, C. R. Chemically tunable mucin chimeras assembled on living cells. *Proc. Natl. Acad. Sci. U. S. A.* **2015**, *112* (41), 12574−12579.
(26) Schellenberger, V.; Wang, C. W.; Geething, N. C.; Spink, B. J.; Campbell, A.; To, W.; Scholle, M. D.; Yin, Y.; Yao, Y.; Bogin, O.; Cleland, J. L.; Silverman, J.; Stemmer, W. P. C. A recombinant polypeptide extends the in vivo half-life of peptides and proteins in a tunable manner. *Nat. Biotechnol.* **2009**, *27* (12), 1186−1155.
(27) Hu, J.; Wang, G. L.; Liu, X. Y.; Gao, W. P. Enhancing pharmacokinetics, tumor accumulation, and antitumor efficacy by elastin-like polypeptide fusion of interferon alpha. *Adv. Mater.* **2015**, *27* (45), 7320−7324.
(28) Luginbuhl, K. M.; Schaal, J. L.; Umstead, B.; Mastria, E. M.; Li, X.; Banskota, S.; Arnold, S.; Feinglos, M.; D'Alessio, D.; Chilkoti, A. One-week glucose control via zero-order release kinetics from an injectable depot of glucagon-like peptide-1 fused to a thermosensitive biopolymer. *Nat. Biomed. Engin.* **2017**, *1*, 0078.

(29) Qin, G. K.; Glassman, M. J.; Lam, C. N.; Chang, D.; Schaible, E.; Hexemer, A.; Olsen, B. D. Topological effects on globular protein-ELP fusion block copolymer self-assembly. *Adv. Funct. Mater.* **2015**, *25* (5), 729−738.

(30) Petitdemange, R.; Garanger, E.; Bataille, L.; Dieryck, W.; Bathany, K.; Garbay, B.; Deming, T. J.; Lecommandoux, S. Selective tuning of elastin-like polypeptide properties via methionine/oxidation. *Biomacromolecules* **2017**, *18* (2), 544−550.

(31) Gomes, S.; Leonor, I. B.; Mano, J. F.; Reis, R. L.; Kaplan, D. L. Natural and genetically engineered proteins for tissue engineering. *Prog. Polym. Sci.* **2012**, *37* (1), 1−17.

(32) Schlapschy, M.; Binder, U.; Borger, C.; Theobald, I.; Wachinger, K.; Kisling, S.; Haller, D.; Skerra, A. PASylation: a biological alternative to PEGylation for extending the plasma half-life of pharmaceutically active proteins. *Protein Eng., Des. Sel.* **2013**, *26* (8), 489−501.

(33) Hou, Y.; Zhou, Y.; Wang, H.; Wang, R.; Yuan, J.; Hu, Y.; Sheng, K.; Feng, J.; Yang, S.; Lu, H. Macrocyclization of interferon-poly(alpha-amino acid) conjugates significantly improves the tumor retention, penetration, and antitumor efficacy. *J. Am. Chem. Soc.* **2018**, *140* (3), 1170−1178.

(34) Yuan, J.; Sun, Y.; Wang, J.; Lu, H. Phenyl trimethylsilyl sulfide-mediated controlled ring-opening polymerization of alpha-amino acid N-carboxyanhydrides. *Biomacromolecules* **2016**, *17* (3), 891−896.

(35) Hou, Y.; Yuan, J.; Zhou, Y.; Yu, J.; Lu, H. A Concise approach to site-specific topological protein-poly(amino acid) conjugates enabled by in-situ generated functionalities. *J. Am. Chem. Soc.* **2016**, *138* (34), 10995−11000.

(36) Zhang, P.; Jain, P.; Tsao, C.; Yuan, Z.; Li, W.; Li, B.; Wu, K.; Hung, H. C.; Lin, X.; Jiang, S. Polypeptides with high zwitterion density for safe and effective therapeutics. *Angew. Chem., Int. Ed.* **2018**, *57* (26), 7743−7747.

(37) Xiong, M.; Lee, M. W.; Mansbach, R. A.; Song, Z.; Bao, Y.; Peek, R. M.; Yao, C.; Chen, L. F.; Ferguson, A. L.; Wong, G. C. L.; Cheng, J. J. Helical antimicrobial polypeptides with radial amphiphilicity. *Proc. Natl. Acad. Sci. U. S. A.* **2015**, *112* (43), 13155−13160.

(38) Lu, H.; Wang, J.; Bai, Y.; Lang, J. W.; Liu, S.; Lin, Y.; Cheng, J. Ionic polypeptides with unusual helical stability. *Nat. Commun.* **2011**, *2*, 206.

(39) Chen, C. Y.; Wang, Z. H.; Li, Z. B. Thermoresponsive polypeptides from pegylated poly-L-glutamates. *Biomacromolecules* **2011**, *12* (8), 2859−2863.

(40) Popp, M. W.; Dougan, S. K.; Chuang, T. Y.; Spooner, E.; Ploegh, H. L. Sortase-catalyzed transformations that improve the properties of cytokines. *Proc. Natl. Acad. Sci. U. S. A.* **2011**, *108* (8), 3169−3174.

(41) Wu, L.; Chen, J. X.; Wu, Y. M.; Zhang, B.; Cai, X. C.; Zhang, Z. W.; Wang, Y.; Si, L. L.; Xu, H.; Zheng, Y. X.; Zhang, C. L.; Liang, C. G.; Li, J.; Zhang, L.; Zhang, Q.; Zhou, D. M. Precise and combinatorial PEGylation generates a low-immunogenic and stable form of human growth hormone. *J. Controlled Release* **2017**, *249*, 84−93.

(42) Cho, H.; Daniel, T.; Buechler, Y. J.; Litzinger, D. C.; Maio, Z.; Putnam, A. M.; Kraynov, V. S.; Sim, B. C.; Bussell, S.; Javahishvili, T.; Kaphle, S.; Viramontes, G.; Ong, M.; Chu, S.; Becky, G. C.; Lieu, R.; Knudsen, N.; Castiglioni, P.; Norman, T. C.; Axelrod, D. W.; Hoffman, A. R.; Schultz, P. G.; DiMarchi, R. D.; Kimmel, B. E. Optimized clinical performance of growth hormone with an expanded genetic code. *Proc. Natl. Acad. Sci. U. S. A.* **2011**, *108* (22), 9060−9065.

(43) Liu, S. Y.; Wei, W.; Yue, H.; Ni, D. Z.; Yue, Z. G.; Wang, S.; Fu, Q.; Wang, Y. Q.; Ma, G. H.; Su, Z. G. Nanoparticles-based multi-adjuvant whole cell tumor vaccine for cancer immunotherapy. *Biomaterials* **2013**, *34* (33), 8291−8300.

(44) Chang, Y. S.; Graves, B.; Guerlavais, V.; Tovar, C.; Packman, K.; To, K. H.; Olson, K. A.; Kesavan, K.; Gangurde, P.; Mukherjee, A.; Baker, T.; Darlak, K.; Elkin, C.; Filipovic, Z.; Qureshi, F. Z.; Cai, H. L.; Berry, P.; Feyfant, E.; Shi, X. G. E.; Horstick, J.; Annis, D. A.;

Manning, A. M.; Fotouhi, N.; Nash, H.; Vassilev, L. T.; Sawyer, T. K. Stapled alpha-helical peptide drug development: a potent dual inhibitor of MDM2 and MDMX for p53-dependent cancer therapy. *Proc. Natl. Acad. Sci. U. S. A.* **2013**, *110* (36), E3445−E3454.

(45) Moellering, R. E.; Cornejo, M.; Davis, T. N.; Del Bianco, C.; Aster, J. C.; Blacklow, S. C.; Kung, A. L.; Gilliland, D. G.; Verdine, G. L.; Bradner, J. E. Direct inhibition of the NOTCH transcription factor complex. *Nature* **2009**, *462* (7270), 182−188.

(46) Walensky, L. D.; Bird, G. H. Hydrocarbon-stapled peptides: principles, practice, and progress. *J. Med. Chem.* **2014**, *57* (15), 6275−6288.

(47) Mochida, Y.; Cabral, H.; Miura, Y.; Albertini, F.; Fukushima, S.; Osada, K.; Nishiyama, N.; Kataoka, K. Bundled assembly of helical nanostructures in polymeric micelles loaded with platinum drugs enhancing therapeutic efficiency against pancreatic tumor. *ACS Nano* **2014**, *8* (7), 6724−6738.

(48) Kierstead, P. H.; Okochi, H.; Venditto, V. J.; Chuong, T. C.; Kivimae, S.; Frechet, J. M. J.; Szoka, F. C. The effect of polymer backbone chemistry on the induction of the accelerated blood clearance in polymer modified liposomes. *J. Controlled Release* **2015**, *213*, 1−9.

(49) van der Eijk, A. A.; Vrolijk, J. M.; Haagmans, B. L. Antibodies neutralizing peginterferon alfa during retreatment of hepatitis C. *N. Engl. J. Med.* **2006**, *354* (12), 1323−1324.

(50) Zhang, C.; Yuan, J.; Lu, J.; Hou, Y.; Xiong, W.; Lu, H. From neutral to zwitterionic poly(alpha-amino acid) nonfouling surfaces: Effects of helical conformation and anchoring orientation. *Biomaterials* **2018**, *178*, 728−737.